



Cite this: *Green Chem.*, 2021, **23**, 2169

Received 20th January 2021,
Accepted 19th February 2021

DOI: 10.1039/d1gc00227a

rs.c.li/greenchem

Synthesis of 1,10-decanediol diacetate and 1-decanol acetate from furfural†

Chen-Qiang Deng, Qin-Zhu Jiang, Jin Deng * and Yao Fu *

A green and efficient method was developed for upgrading furfural to 1,10-decanediol diacetate and 1-decanol acetate. 92% yield of the acetates was obtained through the tandem benzoin condensation and hydrodeoxygenation reaction. During the benzoin condensation, furfural was catalyzed into furoin in a quantitative yield by the immobilized NHC catalyst under solvent-free conditions. After dissolving the furoin intermediate in acetic acid, the Sc(OTf)₃ and Pd/C catalytic system was introduced for hydrodeoxygenation. The effects of reaction factors have been investigated in detail and the hydrodeoxygenation process has been explored by ¹H-NMR and GC-MS.

Introduction

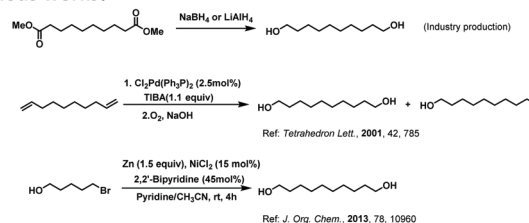
The greenhouse effect and air pollution caused by the excessive consumption of fossil resources have led researchers to explore various forms of renewable resources.¹ As a promising alternative to traditional fossil resources, the abundant lignocellulosic biomass resource is the only renewable organic carbon source.² Furfural, mainly produced from hemicellulose in lignocellulose, is one of the most valuable biomass platform molecules with an annual global production of 100 kton.³ So far, furfural has been developed to convert into many important chemicals, such as furfuryl alcohol,⁴ levulinic acid,⁵ cyclopentanone,⁶ pentanediol,⁷ and 2-methyl tetrahydrofuran.⁸ Therefore, it is of great significance to explore the conversion of furfural into high value-added chemicals.

As an important raw material, 1,10-decanediol is used for the synthesis of surfactants⁹ and ester lubricants¹⁰ in the fine chemicals industry, as well as the production of diiododecane, an important pharmaceutical intermediate.¹¹ Moreover, 1,10-decanediol can be used for the synthesis of membrane materials,¹² heat storage materials,¹³ and various polymer materials.¹⁴ The current industrial production of 1,10-decanediol is obtained by the reduction of sebacic acid (obtained from the oxidation of castor oil) or its esters by using lithium aluminum hydride, sodium borohydride, or other metal-reducing agents.¹⁵ In 2001, Gagneur *et al.*¹⁶ reported the use of dec-

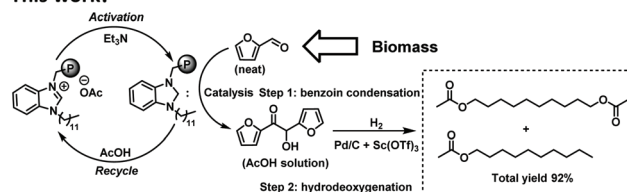
adiene to obtain alkyl aluminum intermediates through the hydrogen transfer and hydroalumination reaction. Then, 1,10-decanediol and 1-decanol were obtained in NaOH under an oxygen atmosphere. In 2013, Peng *et al.*¹⁷ reported the use of 5-bromo-1-pentanol to synthesize 1,10-decanediol by the nickel-catalyzed reductive coupling reaction. However, these methods have many disadvantages, such as the limitation of raw materials, a large number of catalysts, and environmental pollution, and could not meet the requirements of green chemistry. Herein, we describe the synthesis of 1,10-decanediol diacetate and 1-decanol acetate from biomass-derived furfural through a tandem reaction (Scheme 1).

To establish the tandem reaction relationship between furfural and 1,10-decanediol diacetate, we designed a new synthetic route based on retrosynthetic analysis (Scheme 2). 1,10-

Previous works:



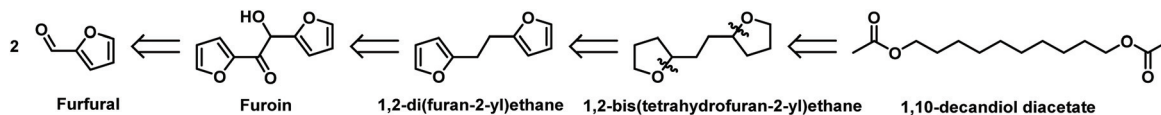
This work:



Scheme 1 Synthesis of 1,10-decanediol/1-decanol and their acetates.

Hefei National Laboratory for Physical Sciences at the Microscale, iChEM, CAS Key laboratory of Urban Pollutant Conversion, Anhui Province Key Laboratory of Biomass Clean Energy, Department of Chemistry, University of Science and Technology of China, Hefei, Anhui 230026, China. E-mail: dengjin@ustc.edu.cn, fuyao@ustc.edu.cn

†Electronic supplementary information (ESI) available. See DOI: 10.1039/d1gc00227a



Scheme 2 The retrosynthetic analysis of 1,10-decanediol diacetate obtained from furfural.

Decanediol diacetate can be obtained by ring-opening and selective hydrogenolysis of 1,2-bis(2-tetrahydrofuryl)ethane, which can be easily obtained by hydrogenation saturation of 1,2-bis(furan-2-yl)ethane. Obviously, the skeleton structure of 1,2-bis(2-tetrahydrofuryl)ethane is highly similar to furoin. Furoin can be readily prepared from biomass-derived furfural through a benzoin condensation reaction. As a powerful catalyst for benzoin condensation, the NHC catalyst was introduced for the first step.¹⁸ On the other hand, because metal triflates can promote the ring-opening of the cyclic ether and Pd/C can achieve the hydrogenation of unsaturated double bonds,¹⁹ the Lewis acids and hydrogenation catalytic system were introduced for the second step. Therefore, the challenges of establishing this method are: (a) controlling the selectivity and sequentiality of hydrodeoxygenation (step 2) and (b) achieving the compatibility of benzoin condensation (step 1) with the reaction pathway of step 2, to realize the synthesis of C₁₀ alcohol esters from biomass-derived furfural.

Results and discussion

Initially, in response to the challenge of selectivity and sequentiality of hydrodeoxygenation (step 2), the effects of metal triflates

on the product distribution were investigated by using furoin as a substrate in an acetic acid system (Table 1). The Lewis acidity of the metal triflate was positively correlated with the charge density on the metal ionic radius.²⁰ Considering that stronger Lewis acidity was beneficial to promote the ring-opening of the cyclic ether, Hf(OTf)₄ and Al(OTf)₃ were preferentially used for the hydrodeoxygenation reaction (entries 1 and 2). Compound **1** was obtained with a yield of 65% and 62%, respectively. On using the medium Lewis acidity of Sc(OTf)₃, 66% yield of **1** was obtained and the total yield was up to 98%. It was demonstrated that Sc(OTf)₃ could effectively activate the ester group and promote the ring-opening of the cyclic ether. However, when the Lewis acidity was further reduced, such as Cu(OTf)₂, the total yield was drastically decreased to 46% (entry 5). Inspired by Chen *et al.*²¹ who reported the preparation of C₁₀–C₁₂ alkanes with the Pd/C and La(OTf)₃ catalytic system, we also investigated lanthanide metal triflates for this reaction (entries 6–16). Unfortunately, none of the lanthanide triflates showed better catalytic activity than Sc(OTf)₃. The relationship between the product distribution and the charge density was not clear. This may be due to the fact that the hydrodeoxygenation reaction is a multi-step series coupling reaction (including the ring-opening of cyclic ethers and the cleavage of esters), which might be affected by many factors simultaneously.

Table 1 The screening of metal triflates in hydrodeoxygenation of furoin

Entry	Metal triflate	Ionic radius	Charge density	Conversion/%	Yield/%			
					1	2	3	Others
1	Hf(OTf) ₄	0.71	5.63	100	65	28	2	5
2	Al(OTf) ₃	0.535	5.61	100	62	30	3	5
3	Sc(OTf)₃	0.745	4.03	100	66	29	3	2
4	Ni(OTf) ₂	0.69	2.90	100	55	16	1	28
5	Cu(OTf) ₂	0.73	2.74	100	36	10	0	54
6	Sm(OTf) ₃	0.958	3.13	100	58	22	1	19
7	Ce(OTf) ₃	1.01	2.97	100	60	21	1	18
8	La(OTf) ₃	1.032	2.91	100	52	19	1	28
9	Yb(OTf) ₃	0.868	3.46	100	50	24	2	24
10	Y(OTf) ₃	0.900	3.33	100	44	17	0	39
11	Lu(OTf) ₃	0.861	3.48	100	61	22	0	17
12	Pr(OTf) ₃	0.99	3.03	100	54	18	1	27
13	Gd(OTf) ₃	0.938	3.20	100	50	13	1	36
14	Ho(OTf) ₃	0.901	3.33	100	43	18	1	38
15	Er(OTf) ₃	0.89	3.37	100	40	15	0	45
16	Dy(OTf) ₃	0.912	3.29	100	44	15	0	41

Reaction conditions: furoin (0.5 mmol), metal triflate (4 mol%), 10% Pd/C (3 mol%), H₂ (3 MPa), acetic acid (10 mL), 180 °C and 6 h. **1**: 1,10-decanediol diacetate; **2**: 1-decanol acetate; **3**: decane; others: including the intermediate product and the product that cannot be detected.

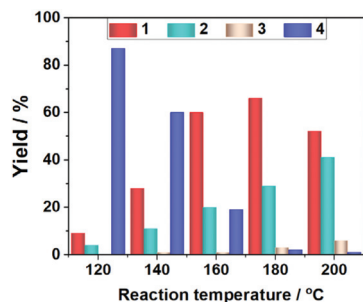


Fig. 1 Effect of the reaction temperature. Reaction conditions: furoin (0.5 mmol), metal triflate (4 mol%), 10% Pd/C (3 mol%), H₂ (3 MPa), acetic acid (10 mL) and 6 h. **1**: 1,10-decanediol diacetate; **2**: 1-decanol acetate; **3**: decane; and **4**: including the intermediate product and the product that cannot be detected.

The reaction temperature was an important factor that affected the ring-opening of cyclic ethers and the cleavage of ester groups. Therefore, the effect of the reaction temperature on the product distribution was investigated (Fig. 1). When the reaction temperature was 120 °C, a lot of hydrogenated intermediates were formed. 13% yield of **1** and **2** was obtained, while **3** was not formed. When the reaction temperature was increased to 160 °C, the hydrogenated intermediate sharply decreased. The yield of **1** and **2** significantly increased to 80%. Meanwhile, a small amount of **3** was detected. The activity of the catalyst increased with the increase of the reaction temperature. When the reaction temperature was 180 °C, a total yield of 98% was obtained. The yield of **1** and **2** increased to 95%. However, when the reaction temperature further increased to 200 °C, the yield of **1** decreased from 66% to 52%, and the yield of **2** increased to 41%. Such results indicated that an excessively high reaction temperature could cause the cleavage of the C–O bonds of **1**. Therefore, the appropriate reaction temperature had an important influence on the selective cleavage of the C–O bonds.

On the other hand, the influence of the hydrogenation catalyst on the hydrodeoxygenation reaction was also investigated (Fig. 2). The 10% Pd/C and 5% Pt/C catalysts had high hydrogenation catalytic activity. Metal triflates could activate the ester group to form a C=C bond which was then saturated by

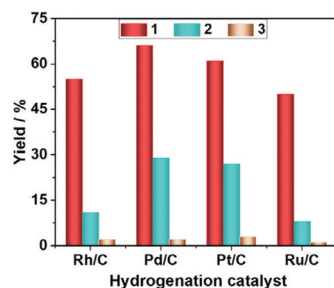


Fig. 2 Effect of the hydrogenation catalyst. Reaction conditions: furoin (0.5 mmol), Sc(OTf)₃ (4 mol%), hydrogenation catalyst (3 mol%), acetic acid (10 mL), H₂ (3 MPa), 180 °C and 6 h. **1**: 1,10-decanediol diacetate, **2**: 1-decanol acetate, and **3**: decane.

the hydrogenation catalyst.²² However, the 5% Ru/C and 5% Rh/C catalysts exhibited relatively weak hydrogenation catalytic activity. Because Ru and Rh had a wide metal d band, the repulsion between the metal surface electron and the C=C bond went against the adsorption of the Ru/C or Rh/C catalyst.²³

After studying the effect of the hydrogenation catalyst on the reaction, we investigated the effect of the hydrogen pressure on the reaction process (Fig. 3). At low hydrogen pressure (1 MPa H₂), 66% yield of **1** and **2** was obtained. With the increase of the hydrogen pressure, the yield of **1** and **2** increased significantly. When the hydrogen pressure reached 3 MPa, **1** and **2** were obtained in 95% yield. However, when the hydrogen pressure further increased from 3 MPa to 4 MPa, the yield of **1** decreased gradually from 66% to 56% and the yield of **2** increased from 28% to 35%. This indicated that high pressure negatively affected the selectivity of compound **1**. Marks and co-workers²⁰ reported that the cracking ability of acetate was related to the stability of the carbocation in the reaction process. The trend for the cleavage of acetate was: tertiary > second > primary. The secondary ester was easier to cleave than the primary ester, so **1** was mainly obtained in the catalytic system. When the hydrogen pressure was too high, the C–O bond of the terminal ester was cleaved. Hence, the optimal hydrogen pressure was 3 MPa.

Next, the effect of the reaction time on the product distribution was explored (Fig. 4). Initially, the reaction mixture was heated to 180 °C for 30 min. Then, it was maintained at 180 °C for a certain time until the reaction was complete. When the reaction mixture was maintained at 180 °C for 30 min, the yields of **1** and **2** were 58% and 20%, respectively. Meanwhile, a small amount of **3** was also detected. This showed that the conversion of the raw material was very fast and Sc(OTf)₃ was an excellent catalyst for the ring-opening of the cyclic ether. With the extension of the reaction time, reaction intermediates gradually decreased, and the total yield of **1** and **2** increased smoothly. When the reaction time was 6 h, the reaction intermediate was almost converted and 95% yield of **1** and **2** was obtained. When the reaction time was extended to 8 h, the yield of **1** decreased slightly, while the yield of **2** and **3** increased further. Overall, the optimal reaction time was 6 h.

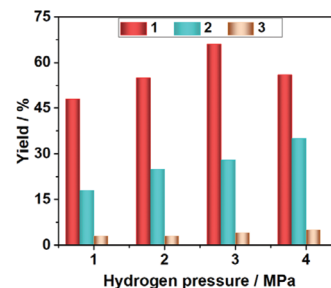


Fig. 3 Effect of the hydrogen pressure. Reaction conditions: furoin (0.5 mmol), Sc(OTf)₃ (4 mol%), 10% Pd/C (3 mol%), acetic acid (10 mL), 180 °C and 6 h. **1**: 1,10-decanediol diacetate, **2**: 1-decanol acetate, and **3**: decane.

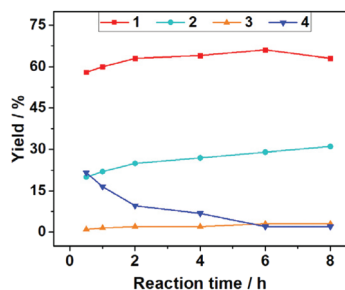


Fig. 4 Effect of the reaction time. Reaction conditions: furoin (0.5 mmol), $\text{Sc}(\text{OTf})_3$ (4 mol%), 10% Pd/C (3 mol%), acetic acid (10 mL), H_2 (3 MPa) and 180 °C. 1: 1,10-decanediol diacetate, 2: 1-decanol acetate, 3: decane, and 4: including the intermediate product and the product that cannot be detected.

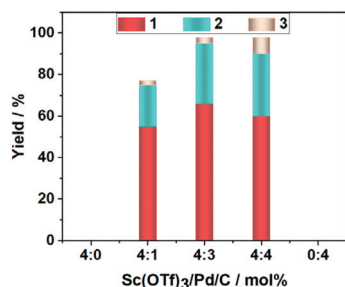


Fig. 5 Effect of the catalyst ratio. Reaction conditions: furoin (0.5 mmol), acetic acid (10 mL), H_2 (3 MPa), 180 °C and 6 h. 1: 1,10-decanediol diacetate, 2: 1-decanol acetate, and 3: decane.

Because the catalytic system consisted of the Lewis acid catalyst and the hydrogenation catalyst, the ratio of $\text{Sc}(\text{OTf})_3$ and Pd/C was investigated (Fig. 5). When $\text{Sc}(\text{OTf})_3$ or Pd/C was used alone, the target product was not obtained. These results indicated that the reaction can only be carried out with both Lewis acid and hydrogenation catalyst. When the catalyst ratio was 4 : 1 (mol%), 79% total yield was obtained. This result revealed that there was a synergistic effect between Pd/C and $\text{Sc}(\text{OTf})_3$. When the catalyst ratio was changed from 4 : 1 to 4 : 3 (mol%), the yield of 1 and 2 significantly increased to 95%. When the catalyst ratio was 4 : 4 (mol%), the yield of 1 decreased slightly, while the yield of 2 and 3 increased further. This indicated that excessive Pd/C would cause over-hydrogenolysis of the C–O bonds of 1. Therefore, the optimal catalyst ratio ($\text{Sc}(\text{OTf})_3/\text{Pd/C}$) was 4 : 3 (mol%).

To further understand the reaction process, $^1\text{H-NMR}$ spectroscopy was performed to monitor the reaction (Fig. 6). The reaction solution with different heating times was characterized by $^1\text{H-NMR}$. The characteristic peaks of the intermediate 1,2-bis(tetrahydrofuran-2-yl)ethane (δ 3.7 ppm) and the product (δ 4.1 ppm, 2.1 ppm, and 0.9 ppm) were observed when heating for 10 min. Meanwhile, the characteristic peaks of the raw material disappeared completely. This indicated that the furan ring was easily hydrogenated during the reaction. With the extension of the heating time, the reaction intermediates gradually decreased. When the reaction solution was heated for 30 min and maintained for 30 min, the character-

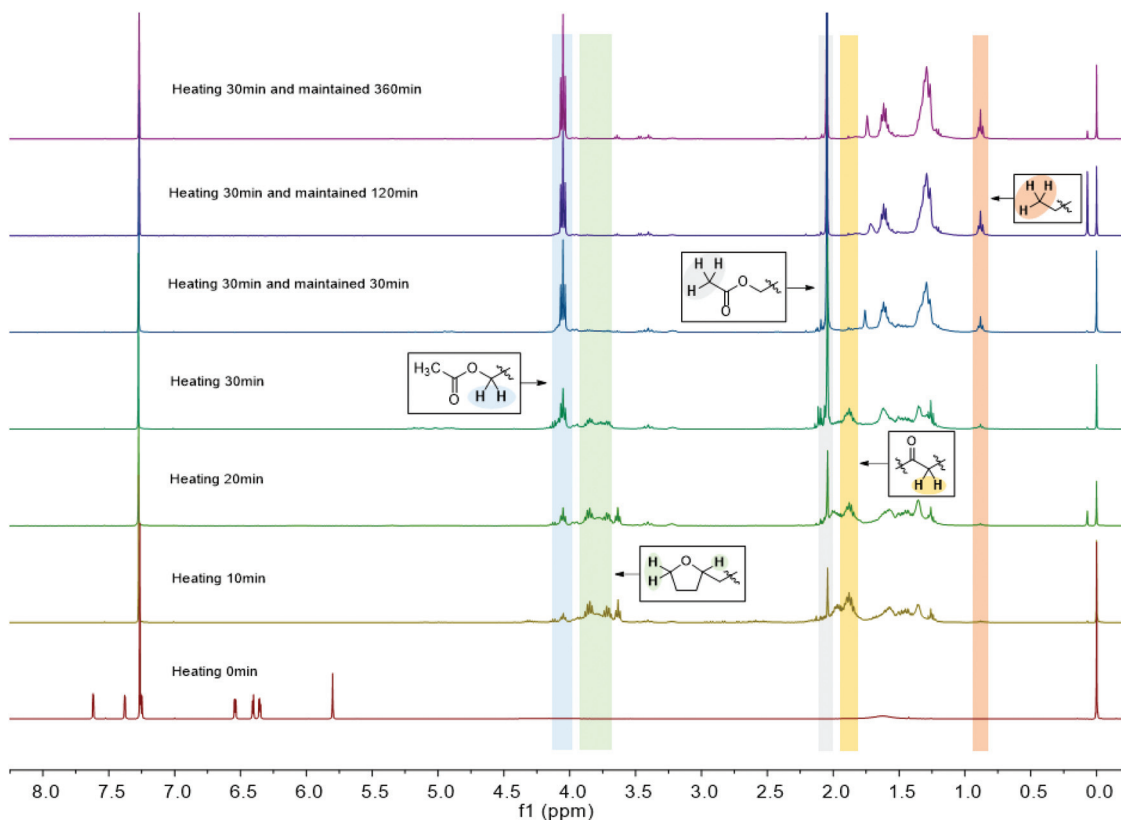
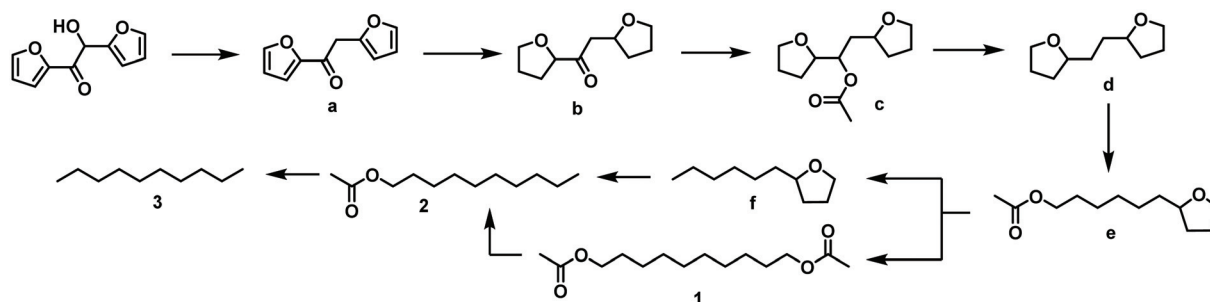


Fig. 6 $^1\text{H-NMR}$ spectra of the reaction solution at different reaction times.



Scheme 3 Proposed reaction mechanism.

istic peak of 1,2-bis(tetrahydrofuran-2-yl)ethane disappeared. Because the characteristic peaks of other intermediates overlapped with those of the product, they could not be distinguished by $^1\text{H-NMR}$. To solve this problem, we used GC-MS to detect the reaction solution heated for 10 min (see the ESI† for details). The GC-MS result showed that the reaction solution had three intermediates: 1,2-bis(tetrahydrofuran-2-yl)ethyl acetate, 1,2-bis(tetrahydrofuran-2-yl)ethane, and 6-(tetrahydrofuran-2-yl)hexyl acetate. Based on the above investigation, we proposed a possible reaction mechanism (Scheme 3). To further verify the reaction pathway, we designed several possible intermediates for the experiment. The results are shown in Table 2. On using 1,2-bis(furan-2-yl)ethane-1,2-diol as the substrate, the target product could not be obtained under standard reaction conditions (Table 2, entry 2). The reason might be that two adjacent hydroxyl groups would coordinate with $\text{Sc}(\text{OTf})_3$, which could not promote the ring-opening of the cyclic ether. However, on using 1,2-di(furan-2-yl)ethan-1-one as the substrate, the target product was obtained in 89% yield (Table 2, entry 3). Such results indicated that the hydroxyl group of furoin was preferentially removed instead of the $\text{C}=\text{O}$ bond being reduced. When intermediate **d** was used as the substrate, 92% yield of the target product was obtained (Table 2, entry 4). This indicated that the reduction of the

$\text{C}=\text{O}$ bond of intermediate **b** preceded the ring-opening of the cyclic ether. Subsequently, the ester group of intermediate **c** was cleaved by Pd/C. Then, intermediate **d** underwent ring-opening *via* metal triflates to obtain intermediate **e**. Finally, the target product was obtained by the ring-opening of the cyclic ether and hydrogenolysis.

According to Scheme 3, intermediate **e** could generate **f** and **1** simultaneously. The ring-opening of intermediate **f** was promoted by metal triflates to obtain **2**. However, **1** could also be over-hydrogenated to form **2**. An attempt was made to optimize the reaction conditions to improve the selectivity of the reaction, but the result was unsatisfactory. The ratio of products **1** to **2** was about 2 : 1 under the optimal reaction conditions. It may be that the formation of **f** and **1** was a parallel reaction, resulting in low selectivity. Although the selectivity of the reaction was not high, the physical properties of products **1** and **2** were quite different. The boiling point difference between **1** (b. p. $136\text{ }^\circ\text{C}$ at 3 mmHg)²⁴ and **2** (b. p. $87\text{ }^\circ\text{C}$ at 3 mmHg)²⁵ was about $50\text{ }^\circ\text{C}$. Thus, products **1** and **2** could be separated through vacuum distillation. The catalytic system has a high application value for the conversion of furfural into fine chemicals.

To test the stability of the Pd/C catalyst, a recycling experiment was conducted. Biphenyl was added to the reaction solution for quantitative product analysis. The reaction mixture was centrifuged to collect Pd/C, which was then dried and used for the next cycle. Fig. 7 shows the results of the Pd/C recycling experiment. The catalytic activity decreased slightly

Table 2 Possible intermediates as substrates used to verify the reaction pathway

Entry	Substrate	Yield/%			Total
		1	2	3	
1		66	29	3	98
2		4	1	0	5
3		57	32	3	92
4		52	40	5	97

Reaction conditions: furoin (0.5 mmol), metal triflate (4 mol%), 10% Pd/C (3 mol%), H_2 (3 MPa), acetic acid (10 mL), $180\text{ }^\circ\text{C}$ and 6 h. **1**: 1,10-decanediol diacetate; **2**: 1-decanol acetate; **3**: decane; total: sum of **1**, **2**, and **3**.

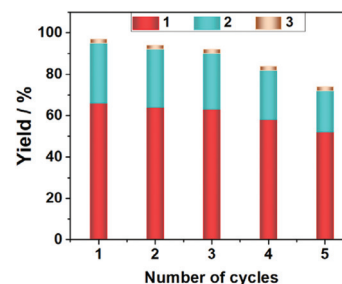


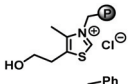
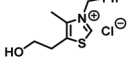
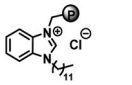
Fig. 7 Recycling study. Reaction conditions: furoin (0.5 mmol), $\text{Sc}(\text{OTf})_3$ (4 mol%), acetic acid (10 mL), H_2 (3 MPa), $180\text{ }^\circ\text{C}$ and 6 h. **1**: 1,10-decanediol diacetate, **2**: 1-decanol acetate, and **3**: decane.

after three cycles. The Pd/C catalyst certainly showed stability. However, the catalytic activity of the Pd/C catalyst decreased sharply at the fifth run. We analyzed the used Pd/C after 5 cycles by transmission electron microscopy (TEM) characterization. The used Pd/C was partially agglomerated in contrast with the fresh Pd/C (see the ESI† for details). This indicated that the decrease of catalytic activity was connected with the formation of Pd agglomerates on the Pd/C catalyst.¹⁹ Besides, the loss and oxidation of the catalyst during the recovery process in the air also contributed to a decrease in the yield.

After completing the optimization of step 2, for the benzoin condensation (step 1), we decided to use a green NHC catalyst with high catalytic activity. However, the NHC catalyst usually needs to be converted into an active carbene form by alkaline reagents, and the carbene form is unstable and easily destroyed in the air. What was more difficult was that because the subsequent hydrodeoxygenation (step 2) was carried out in acetic acid, the reaction conditions of the sequential two steps were incompatible. To achieve the compatibility of the two steps, the strategies including solvent-free reaction conditions and catalyst immobilization were applied in step 1. Consequently, at the end of step 1, the furoin product could be dissolved in acetic acid to obtain the reaction solution of step 2. Meanwhile, the NHC catalyst could be recovered and transformed from unstable carbene into stable acetate. Based on the above assumption, a one-pot, two-step tandem method was established to prepare 1,10-decanediol and 1-decanol acetates from furfural.

Initially, inspired by the vitamin B1 catalyst, we prepared a thiazole-type immobilized NHC catalyst by immobilizing 2-(4-methylthiazol-5-yl)ethan-1-ol on Merrifield resin to catalyze benzoin condensation. 0.5 mol% thiazole-type immobilized NHC catalyzed furfural condensation to obtain furoin in 98% yield under solvent-free conditions. Subsequently, acetic acid was added to the product. The acetic acid solution was filtered to remove the thiazole-type immobilized NHC catalyst, and then the hydrodeoxygenation reaction was carried out under standard conditions (Table 3, entry 1). Unfortunately, the

Table 3 Furoin from different sources for the hydrodeoxygenation reaction^a

Entry	NHC catalyst	Substrate	Yield/%			
			1	2	3	Total
1		Furoin ^b	3	0	0	3
2		Furoin ^c	2	0	0	2
3	—	Furoin ^c	66	29	3	98
4		Furoin ^b	65	27	2	94

^a 0.5 mol% NHC catalyst (entries 1 and 4) and 0.1 mol% NHC catalyst (entry 2). ^b Furoin was prepared from furfural with the NHC catalyst. ^c Commercially available furoin. 1: 1,10-decanediol diacetate; 2: 1-decanol acetate; 3: decane; total: sum of 1, 2, and 3.

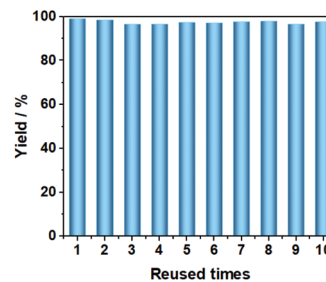


Fig. 8 Reused times of the imidazole-type immobilized NHC catalyst.

target product was not obtained. We speculated that the thiazole-type immobilized NHC catalyst containing the S element may poison the Pd/C catalyst. To prove this speculation, we used commercially available furoin as the substrate. 0.1 mol% thiazole-type non-immobilized NHC catalyst was added to the reaction system and the hydrodeoxygenation reaction was carried out under standard conditions (Table 3, entry 2). Similarly, the target product was not obtained. The result was consistent with our speculation. Therefore, we considered using an imidazole-type immobilized NHC catalyst for step 1. The preparation of the imidazole-type immobilized NHC catalyst was performed by immobilizing 1-undecyl-1*H*-benzo[*d*]imidazole on Merrifield resin. 0.5 mol% imidazole-type immobilized NHC catalyst achieved almost full condensation of furfural to furoin under solvent-free conditions. The hydrodeoxygenation reaction was then carried out under standard conditions (Table 3, entry 4). 92% yield of the target product was obtained, which was consistent with commercially available furoin as the substrate (Table 3, entry 3). These results confirmed that the S element in the thiazole-type immobilized NHC catalyst could cause the deactivation of the Pd/C catalyst. Finally, the reusability of the immobilized NHC catalyst was tested. Both types of immobilized NHC catalysts had high catalytic activity and stability. The activity of the catalyst did not decrease after 10 cycles (Fig. 8 and Fig. S2†). In short, tandem benzoin condensation (step 1) and hydrodeoxygenation (step 2) realized the synthesis of 1,10-decanediol diacetate and 1-decanol acetate from biomass-derived furfural.

Conclusions

In summary, the synthesis of 1,10-decanediol diacetate and 1-decanol acetate was achieved from biomass-derived furfural through benzoin condensation to obtain furoin under solvent-free conditions with the immobilized NHC catalyst followed by selective hydrodeoxygenation with the Sc(OTf)₃ and Pd/C co-catalytic system in acetic acid. This method realized the conversion of biomass-derived molecules into high value-added chemicals. Up to 92% yield of 1,10-decanediol and 1-decanol acetates was obtained by the tandem benzoin condensation and hydrodeoxygenation reaction. The immobilized NHC catalysts have high catalytic activity and stability. This tandem reac-

tion provides a green and efficient method for the synthesis of C₁₀ alcohol esters from biomass platform molecules.

Author contributions

Chen-Qiang Deng: data curation, investigation, formal analysis, and writing – original draft; Qin-Zhu Jiang: investigation and writing – original draft; Yao Fu: resources and supervision; Jin Deng: conceptualization, methodology, project administration, resources, supervision, and writing – review and editing.

Conflicts of interest

There are no conflicts to declare.

Acknowledgements

This work was financially supported by the National Key R&D Program of China (2018YFB1501502), the National Natural Science Foundation of China (21875239), and the Fundamental Research Funds for the Central Universities (WK3530000004). The authors thank Hefei Leaf Biotech Co., Ltd and Anhui Kemi Machinery Technology Co., Ltd for free samples and equipment that benefited their ability to conduct this study.

Notes and references

- (a) A. Corma, S. Iborra and A. Velty, *Chem. Rev.*, 2007, **107**, 2411–2502; (b) X. D. Li, P. Jia and T. F. Wang, *ACS Catal.*, 2016, **6**, 7621–7640.
- (a) G. W. Huber and A. Corma, *Angew. Chem., Int. Ed.*, 2007, **46**, 7184–7201; (b) H. Li, A. Riisager, S. Saravanamurugan, A. Pandey, R. S. Sangwan, S. Yang and R. Luque, *ACS Catal.*, 2018, **8**, 148–187; (c) D. M. Alonso, S. G. Wettstein and J. A. Dumesic, *Green Chem.*, 2013, **15**, 584–595; (d) Y. B. Huang, Y. J. Luo, A. Del Rio Flores, L. C. Li and F. Wang, *ACS Sustainable Chem. Eng.*, 2020, **8**, 12161–12167; (e) X. L. Li, K. Zhang, J. L. Jiang, R. Zhu, W. P. Wu, J. Deng and Y. Fu, *Green Chem.*, 2018, **20**, 362–368.
- J. J. Bozell and G. R. Petersen, *Green Chem.*, 2010, **12**, 539–554.
- (a) Z. R. Zhang, J. L. Song, Z. W. Jiang, Q. L. Meng, P. Zhang and B. X. Han, *ChemCatChem*, 2017, **9**, 2448–2452; (b) M. G. Dohade and P. L. Dhepe, *Green Chem.*, 2017, **19**, 1144–1154; (c) Y. T. Wang, P. Prinsen, K. S. Triantafyllidis, S. A. Karakoulia, A. Yopez, C. Len and R. Luque, *ChemCatChem*, 2018, **10**, 3459–3468.
- (a) A. D. Dwivedi, K. Gupta, D. Tyagi, R. K. Rai, S. M. Mobin and S. K. Singh, *ChemCatChem*, 2015, **7**, 4050–4058; (b) A. D. Dwivedi, V. K. Sahu, S. M. Mobin and S. K. Singh, *Inorg. Chem.*, 2018, **57**, 4777–4787.
- (a) Q. Deng, R. Cao, X. Li, J. Wang, Z. L. Zeng, J. J. Zou and S. G. Deng, *ACS Catal.*, 2020, **10**, 7355–7366; (b) G. S. Zhang, M. M. Zhu, Q. Zhang, Y. M. Liu, H. Y. He and Y. Cao, *Green Chem.*, 2016, **18**, 2155–2164.
- (a) W. J. Xu, H. F. Wang, X. H. Liu, J. W. Ren, Y. Q. Wang and G. Z. Lu, *Chem. Commun.*, 2011, **47**, 3924–3926; (b) Q. Y. Liu, B. T. Qiao, F. Liu, L. L. Zhang, Y. Su, A. Q. Wang and T. Zhang, *Green Chem.*, 2020, **22**, 3532–3538; (c) S. Liu, Y. Amada, M. Tamura, Y. Nakagawa and K. Tomishige, *Catal. Sci. Technol.*, 2014, **4**, 2535–2549; (d) L. Gavilà, A. Lähde, J. Jokiniemi, M. Constanti, F. Medina, E. del Río, D. Tichit and M. G. Alvarez, *ChemCatChem*, 2019, **11**, 4944–4953; (e) R. Zhu, G. Y. Zhou, B. X. Gong, J. Deng and Y. Fu, *Appl. Catal., A*, 2020, **608**, 117888–117896.
- (a) F. Dong, Y. L. Zhu, G. Q. Ding, J. L. Cui, X. Q. Li and Y. W. Li, *ChemSusChem*, 2015, **8**, 1534–1537; (b) J. G. Stevens, R. A. Bourne, M. V. Twigg and M. Poliakoff, *Angew. Chem., Int. Ed.*, 2010, **49**, 8856–8859; (c) Y. B. Huang, A. F. Liu, Q. Zhang, K. M. Li, W. B. Porterfield, L. C. Li and F. Wang, *ACS Sustainable Chem. Eng.*, 2020, **8**, 11477–11490.
- R. A. Harris, H. van der Walt and P. M. Shumbula, *J. Mol. Struct.*, 2013, **1048**, 18–26.
- O. Fandiño, J. García, M. J. P. Comuñas, E. R. López and J. Fernández, *Ind. Eng. Chem. Res.*, 2006, **45**, 1172–1182.
- (a) L. E. Craig and D. S. Tarbell, *J. Am. Chem. Soc.*, 1948, **70**, 2783–2785; (b) Y. T. He, H. N. Yang and Z. J. Yao, *Tetrahedron*, 2002, **58**, 8805–8810.
- F. Pithan and C. Staudt-Bickel, *ChemPhysChem*, 2003, **4**, 967–973.
- W. D. Li and E. Y. Ding, *Mater. Lett.*, 2007, **61**, 4325–4328.
- (a) S. Y. Xu, F. Wu, Z. K. Li, X. Zhu, X. H. Li, L. Wang, Y. J. Li and Y. F. Tu, *Polymer*, 2019, **178**, 121591–121597; (b) K. L. Hu, D. P. Zhao, G. L. Wu and J. B. Ma, *Polym. Chem.*, 2016, **7**, 1096–1110.
- (a) R. G. Jones, *J. Am. Chem. Soc.*, 1947, **10**, 2350–2354; (b) Y. N. Xu and Y. Y. W, *Synth. Commun.*, 2010, **40**, 3423–3429.
- S. Gagneur, H. Makabe and E. Negishi, *Tetrahedron Lett.*, 2001, **42**, 785–787.
- Y. Peng, L. Luo, C. S. Yan, J. J. Zhang and Y. W. Wang, *J. Org. Chem.*, 2013, **78**, 10960–10967.
- (a) D. J. Liu and E. Y.-X. Chen, *ACS Catal.*, 2014, **4**, 1302–1310; (b) W. Lu and E. Y.-X. Chen, *ACS Catal.*, 2015, **5**, 6907–6917; (c) J. Wilson and E. Y.-X. Chen, *ACS Sustainable Chem. Eng.*, 2016, **4**, 4927–4936.
- (a) X. Y. Liu, Y. B. Li, J. Deng and Y. Fu, *Green Chem.*, 2019, **21**, 4532–4540; (b) K. Zhang, X. L. Li, S. Y. Chen, H. J. Xu, J. Deng and Y. Fu, *ChemSusChem*, 2018, **11**, 726–734; (c) Y. B. Li, H. Y. Guo, C. Q. Deng and J. Deng, *Green Energy Environ.*, 2021, DOI: 10.1016/j.jee.2020.11.001.
- (a) T. L. Lohr, Z. Li, R. S. Assary, L. A. Curtiss and T. J. Marks, *Energy Environ. Sci.*, 2016, **9**, 550–564; (b) Z. Li, R. S. Assary, A. C. Atesin, L. A. Curtiss and T. J. Marks, *J. Am. Chem. Soc.*, 2014, **136**, 104–107.

- 21 D. J. Liu and E. Y.-X. Chen, *ChemSusChem*, 2013, **6**, 2236–2239.
- 22 R. Zhu, J. L. Jiang, X. L. Li, J. Deng and Y. Fu, *ACS Catal.*, 2017, **7**, 7520–7528.
- 23 U. K. Singh and M. A. Vannice, *Appl. Catal., A*, 2001, **213**, 1–24.
- 24 V. V. Gromova, *J. Appl. Chem. USSR (Engl. Transl.)*, 1967, **62**, 98–99.
- 25 S.-M. Seo, J. Kim, E. Kim, H.-M. Park, Y.-J. Kim and I. I.-K. Park, *J. Agric. Food Chem.*, 2010, **58**, 1823–1827.